Malaysian Journal of Chemistry, 2022, Vol. 24(2), 120-130
(Special Issue: *2nd IKM Pahang Branch Symposium 2022 – Sustainability & Diversity Through Chemistry*)

Molecular Docking and ADME Profiling of Xanthorrhizol Derivatives as Hyaluronidase Inhibitors

Tengku Kamilah Tengku Nazmi, Nurul Iman Aminudin* and Nurasyikin Hamzah
Department of Chemistry, Kulliyyah of Science, International Islamic University Malaysia (IIUM), 25200, Kuantan, Pahang, Malaysia
*Corresponding author (e-mail: nuruliman@iium.edu.my)

Hyaluronidase (Hyal) enzyme is a potential biological target for the development of anti-inflammatory agents. Xanthorrhizol, a bisabolene sesquiterpenoid isolated from *Curcuma xanthorrhiza* has been reported to show anti-inflammatory activity against cyclooxygenase (COX), inducible nitric oxide synthase (iNOS), and interleukins (IL). However, the activity of xanthorrhizol as a Hyal inhibitor has not been exploited. In this study, a total of 26 xanthorrhizol derivatives with structural modifications at the R_1 - R_4 scaffold were chosen. Molecular docking was performed to virtually screen their structure-activity relationships towards Hyal, while ADME prediction was done to predict their pharmacokinetic profiles. All derivatives bound to the active site of Hyal1 with binding energies ranging from -5.7 kcal/mol to -8.5 kcal/mol. Derivatives **24** and **14** with a benzyloxy moiety at position R_1 and polar moieties at positions R_3 and R_4 showed lower binding energies (-8.3, and -7.9 kcal/mol, respectively) compared to apigenin, **28** (-7.9 kcal/mol) and xanthorrhizol, **1** (-6.5 kcal/mol). These derivatives also fulfilled all ADME and drug-likeness properties, indicating they were potential Hyal inhibitors. Through this work, the activity of xanthorrhizol derivatives against Hyal1 may be predicted and screened as a basis for future modifications of xanthorrhizol to create a potential Hyal inhibitor.

Key words: Xanthorrhizol; hyaluronidase; Molecular Docking; ADME Profile

Received: December 2021; Accepted: February 2022

Inflammation is a result of the immune system's response to maintain the integrity of the human body after exposure to pathogens/toxic compounds or external injury, which involves various signalling molecules and nuclear transcription pathways [1]. Chronic inflammation such as rheumatoid arthritis and cancers can occur when disruption or failure occurs during the acute inflammatory response [2]. Many enzymes are responsible for the regulation of inflammation response, and one of them is hyaluronidase (Hyal). Hyal is a glycoside hydrolase enzyme responsible for the degradation of hyaluronic acid (HA), a major constituent of the extracellular matrix (ECM). In the human body, six isozymes were found to be expressed in different body parts, including liver, testes, uterus, skin, and body fluids like tears and semen [3]. Among them, hyaluronidase-1 and hyaluronidase-2 are the two key enzymes responsible for the degradation of HA [4]. HA degradation results in the production of low molecular weight HA (LMW-HA) fragments, which can induce inflammatory and immunosuppressive responses [5]. This is due to the ability of the fragments to trigger the action of inducible nitric oxide synthase (iNOS) in macrophage cell lines. In addition, it stimulates dendritic and endothelial signalling pathways, leading to the production of various inflammatory cytokines such as interleukins (IL)-1β, IL-12, and tumour necrosis factor-α (TNF-α) [6]. As a result, Hyal is a suitable target for developing anti-inflammatory agents.

Curcuma xanthorrhiza, or "temulawak", is a native plant of Indonesia which is widely distributed in other countries including Malaysia, Thailand and the Philippines. Also known as *"Javanese turmeric", C. xanthorrhiza* is a popular ingredient in traditional health supplements or "jamu" [7]. Traditional uses of *C. xanthorrhiza* also extend to the treatment of inflammation-related diseases like wound healing, hepatitis and rheumatism [8]. The health benefits of *C. xanthorrhiza* are attributed to secondary metabolites that can be found in the plant. Xanthorrhizol **(1)**, a type of bisabolene sesquiterpenoids, is found abundantly as an active compound in the rhizome part of *C. xanthorrhiza* essential oil [9] and extract [7]. It was reported that xanthorrhizol possessed a wide range of biological effects, including anti-bacterial [10, 11], anti-oxidant [12], anti-hyperglycemic [13], and anti-cancer [14] activities. Moreover, xanthorrhizol also exhibits anti-inflammatory activities through inhibition of several enzymes and inflammatory mediators that contribute to inflammation, like cyclooxygenase (COX), inducible nitric oxide synthase (iNOS) [15,16], and interleukins (IL) [17]. Although substantial research has been conducted on xanthorrhizol's biological activities, particularly its anti-inflammatory effects, there have been no reports of its activity against the Hyal enzyme.

†Paper presented at the 2nd IKM Pahang Branch Symposium 2022 – Sustainability & Diversity Through Chemistry

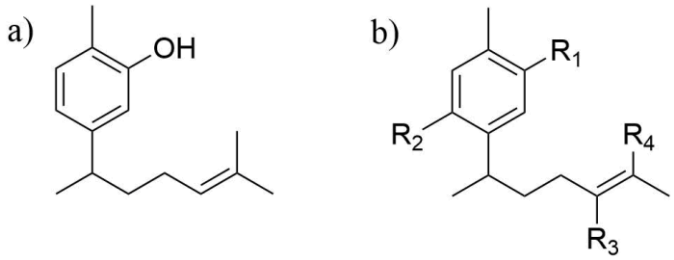

Figure 1. a) Structure of xanthorrhizol, **1**; b) Chemical modification at R_1-R_4.

Xanthorrhizol has one benzene ring, one phenolic hydroxyl group *ortho* to the methyl group and an alkene moiety on the alkyl side chain *para* to the methyl group (Figure 1a). There are a number of reports on the synthesis of xanthorrhizol derivatives by chemical modification of the three moieties represented by R_1-R_4 (Figure 1b) [18, 19, 20, 21]. Despite extensive research, to date, there have been no reports on the structure-activity relationship (SAR) of these derivatives towards the Hyal enzyme. A common approach to SAR involves two steps: design of the drug through the synthesis of the derivatives, followed by *in vitro* enzymatic or cell biology assays. However, this approach requires extensive synthesis of many derivatives that are normally not targeted towards a specific protein. It usually takes time, is costly and may be less accurate. Moreover, the design of drugs at the early stage usually ignores the pharmacokinetic profile for absorption, distribution, metabolism and excretion (ADME) of the drug in the body, leading to the failure of almost 50 % of potential drug candidates [22]. *In silico* approaches such as molecular docking and ADME prediction are now preferred [23]. Molecular docking can predict the binding affinity between the designed drug and the target protein; thus, it is more targeted [24]. On the other hand, predicting the pharmacokinetic profile using SwissADME tools by the Swiss Institute of Bioinformatics [25] provides critical information regarding the potential of the molecule to be developed as a drug [26]. In this study, a small library containing 26 xanthorrhizol derivatives was virtually screened using molecular docking targeting the Hyal enzyme. The SAR of the selected derivatives at R_1 - R_4 positions were determined by analyzing their binding energies and interactions with the amino acid residues. The ADME profiles and drug-likeness properties of the derivatives were also assessed to establish their efficiency and efficacy against the Hyal enzyme.

MATERIALS AND METHODS

Ligand Preparation

Xanthorrhizol (**1**), 26 selected xanthorrhizol derivatives (**2-27**) and apigenin (**28**) were chosen as ligands for this work. The structures of all ligands shown in Figure 1 were sketched with ChemDraw 15.0 [27] to generate its SMILE notations. All 3D structures of the ligands were generated and optimized using the AutoOptimize tool in Avogadro 2.0 [28]. The optimized ligands were saved in PDB format for use in AutoDockTools (ADT) 1.5.6 [29] to compute the Gasteiger charges. The ligands with charges were then saved in PDBQT format for molecular docking.

Protein Preparation

Human hyaluronidase-1 (Hyal1) was selected as the target enzyme. The crystal structure of the protein (PDB ID: 2PE4) with a resolution of 2.0 Å was obtained from the Protein Data Bank (https: //rcsb.org). Water molecules and bound ligands were removed with PyMOL, before the addition of polar hydrogen atoms and Kollman charges using ADT 1.5.6. The optimized protein was then saved in PDBQT format for molecular docking.

Grid Box Preparation

The grid box was created with AutoGrid in ADT 1.5.6 to cover all the amino acid residues at the active site [30]. The grid box dimensions were specified at 62, 58 and 58 Å (x, y, z axes, respectively) and centred at 37.045, -17.292, -11.844 (x, y, z axes, respectively).

Molecular Docking

AutoDock Vina [31] was used as the docking program in this study. The configuration file was prepared according to the grid box set previously defined, and the number of modes was set to 20 runs. Upon completion of the docking simulation, the results were visualized using PyMOL and Discovery Studios for 3D and 2D representations, respectively.

In silico ADME Profiling

The *in silico* ADME profiles for all ligands were evaluated using the SwissADME server (http://www. swissadme.ch/) by the Swiss Institute of Bio-informatics [25]. The SMILES notations generated during ligand preparation were submitted to the server for ADME evaluation.

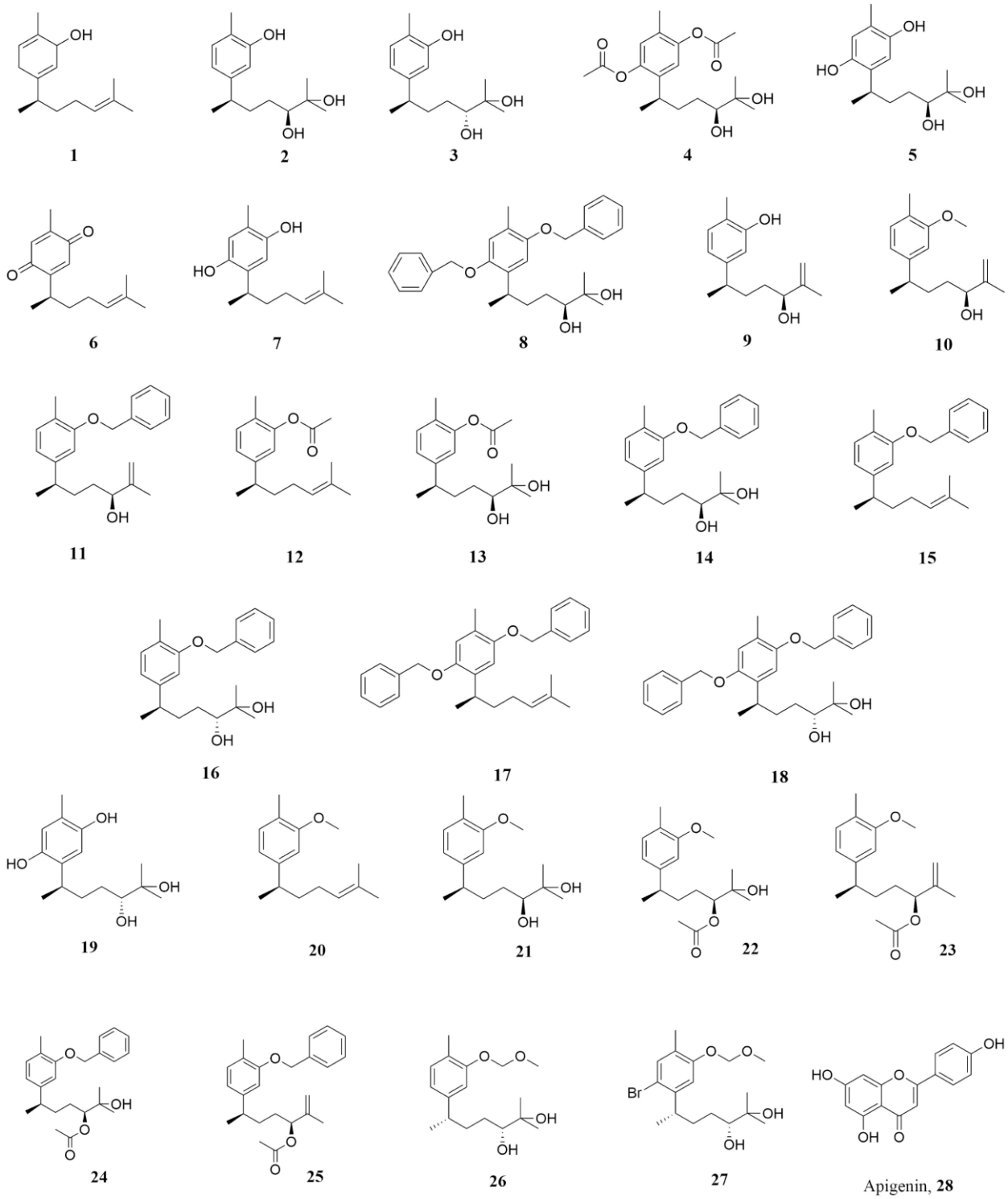

Figure 2. 2D structures of all ligands.

RESULTS AND DISCUSSION

Molecular Docking Studies

Xanthorrhizol is the major active compound found in *C. xanthorrhiza*, which differentiates it from other *Curcuma* species [32]. The structure of xanthorrhizol, **1**, can be modified through chemical synthesis to produce its derivatives. In this study, 26 xanthorrhizol derivatives with known chemical synthesis methods [18, 19] were selected as the starting point for further virtual screening. As the synthesis, characterization and enzymatic assays would be time-consuming, the derivatives' activities against Hyal1 were virtually screened using molecular docking studies. Apigenin, **28**, a positive control in the hyaluronidase enzyme inhibitory assay and known

Hyal inhibitor [33], was used as the reference compound for the docking studies.

Table 1 lists the free binding energies exhibited by all ligands ranked from lowest to highest energy and the amino acid residues involved in the binding interactions. Overall, all derivatives showed free binding energies ranging from -5.7 to -8.5 kcal/mol. Among those, seven derivatives (**17**, **8**, **18**, **24**, **25**, **11**, and **15**) had binding energies (> -8.0 kcal/mol) which were lower than apigenin (-7.9 kcal/mol) and xanthorrhizol (-6.5 kcal/mol). Derivative **14** had the same binding energy value as apigenin.

Table 1. Docking results of xanthorrhizol derivatives against Hyal1 enzyme.

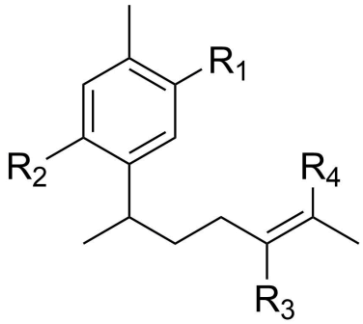

Derivatives	Substituent	Free binding energy (kcal/mol)	Interacting amino acid residues
17	R_1-OBz, R_2-OBz, R_3-H, R_4- CH_3,	-8.5	Ile73, **Asp129**, **Glu131**, Tyr247, Tyr286, Trp321
8	R_1-OBz, R_2-OBz, R_3-(*S*)-OH, R_4-OH	-8.3	**Asp129**, **Glu131**, Tyr202, Tyr210, Tyr286, Trp321
18	R_1-OBz, R_2-OBz, R_3-(*R*)-OH, R_4-OH	-8.3	Ile73, **Asp129**, **Glu131**, Tyr286, Trp321
24	R_1-OBz, R_2-H, R_3-OH, R_4-Ac	-8.3	Ile73, **Asp129**, **Glu131**, Gly203, Tyr210, Ser245, Tyr286, Trp321
25	R_1-OBz, R_2-H, R_3-H, R_4-Ac	-8.2	Ile73, Val127, **Asp129**, **Glu131**, Gly203, Tyr247, Arg265, Tyr286, Asp292, Trp321
11	R_1-OBz, R_2-H, R_3-OH, R_4-CH_2	-8.0	Ile73, **Asp129**, **Glu131**, Tyr202, Tyr286, Trp321
15	R_1-OBz, R_2-H, R_3-H, R_4-CH_3	-8.0	Pro62, Ile73, **Asp129**, **Glu131**, Tyr247, Tyr286, Trp321
14	R_1-OBz, R_2-H, R_3-(*S*)-OH, R_4-OH	-7.9	Ile73, **Asp129**, **Glu131**, Tyr202, Ser245, Tyr286, Trp321
28 (Apigenin)	-	-7.9	Trp130, **Glu131**, Tyr202, Tyr210, Ser245, Arg265, Tyr261
16	R_1-OBz, R_2-H, R_3-(*R*)-OH, R_4-OH	-7.6	**Asp129, Glu131**, Tyr202, Tyr247, Tyr286
12	R_1- Ac, R_2-H, R_3-H, R_4-CH_3	-6.9	Tyr75, **Asp129**, **Glu131**, Tyr202, Trp321
13	R_1- Ac, R_2-H, R_3-OH, R_4-OH	-6.7	Tyr75, **Asp129**, **Glu131**, Trp321
3	R_1-OH, R_2-H, R_3-(*R*)-OH, R_4-OH	-6.6	Asn37, Ile73, Tyr75, Val127, **Asp129**, Tyr202, Tyr286, Trp321
4	R_1- Ac, R_2-Ac, R_3-OH, R_4-OH	-6.6	**Glu131**, Tyr202, Ser245, Tyr247
7	R_1-OH, R_2-OH, R_3-H, R_4-CH_3	-6.6	Pro62, Tyr202, Tyr286, Trp321, Val322, Trp324
1 (Xanthorrhizol)	R_1-OH, R_2-H, R_3-H, R_4-CH_3	-6.5	Arg134, Tyr210, Pro249, Tyr261
2	R_1-OH, R_2-H, R_3-(*S*)-OH, R_4-OH	-6.5	Ile73, Tyr75, Val127, **Asp129**, **Glu131**, Tyr202, Tyr286, Trp321
6	R_1- CO, R_2-CO, R_3-H, R_4-H	-6.5	Tyr202, Tyr286, Trp321, Trp324

9	R_1-OH, R_2-H, R_3-OH, R4-CH_2	-6.5	Ile73, Tyr75, **Asp129**, Tyr202, Tyr286, Asp292, Trp321
19	R_1-OH, R_2-OH, R_3-OH, R_4-OH	-6.4	**Asp129**, **Glu131**, Tyr202, Ser245, Tyr247, Trp321
20	R_1-OMe, R_2-H, R_3-H, R_4-CH_3	-6.3	Tyr75, **Asp129**, Tyr202, Trp321
22	R_1-OMe, R_2-H, R_3-Ac, R_4-OH	-6.3	Pro62, **Glu131**, Tyr247
23	R_1-OMe, R_2-H, R_3-Ac, R_4-CH_2	-6.3	Pro62, Trp321
26	R_1-OMOM, R_2-H, R_3-OH, R_4-OH	-6.2	Arg134, Gly203, Asp206, Tyr210
21	R_1-OMe, R_2-H, R_3-OH, R_4-OH	-6.4	Tyr75, **Asp129**, **Glu131**, Tyr202, Asp292, Trp321
10	R_1-OMe, R_2-H, R_3-OH, R_4-CH_2	-6.1	Tyr75, **Asp129**, **Glu131**, Asp292, Trp321
27	R_1-OMOM, R_2-Br, R_3-OH, R_4-OH	-6.1	Tyr75, **Asp129**, **Glu131**, Tyr202, Tyr286, Trp321
5	R_1-OH, R_2-OH, R_3-OH, R_4-OH	-5.7	Asn37, Tyr75, **Asp129**, **Glu131**, Tyr247, Tyr286

*(OBz= benzyloxy, Ac = acetate, OMe = methoxy, OMOM= methoxymethyl ether, OH = hydroxyl, H = hydrogen)

All derivatives were able to dock at the active site of Hyal1 as visualized using PyMOL and Discovery Studio (Figure 3a). Xanthorrhizol was found to interact with Arg134, Tyr210, Pro249, and Tyr261 residues (Figure 3b), and formed hydrogen bonds with Tyr261. It also interacted with Arg134 and Pro249 through pi-alkyl interactions and Tyr210 through pi-hydrogen bond interactions. Derivative **17**, with benzyloxy moieties at R_1 and R_2 positions (Figure 2), exhibited the lowest binding affinity (-8.5 kcal/mol) among all ligands. Figure 3(c) depicts the interactions of **17** with the amino acid residues at the active site of Hyal1. The aromatic ring from the xanthorrhizol scaffold and benzyloxy at the R_1 position of ligand **17** interacted with Asp129 and Glu131 *via* pi-anion interactions, but no interaction was observed for the benzyloxy substituent at R_2. A similar docking pattern with derivatives was also observed for derivatives **8** and **18**.

Asp129 and Glu131 are two known important active site amino acid residues in the Hyal1 protein. The mutation of Glu131 to other amino acid residues eliminated all activity in Hyal1, while Asp129 mutation also reduced the enzyme activity [34], suggesting the importance of these residues in the enzyme mechanism. Both amino acid residues were also involved in the catalytic cleavage of the β1-4 linkage of *N*-acetylglucosamine and glucuronic acid of HA polymers [34]. Hence, interactions with these two residues may block the Hyal1 action in the degradation of HA. Additionally, the aromatic ring in the benzyloxy moiety of R_1 in derivative **17** also interacted with Tyr286 through pi-donor hydrogen bonding, while the aromatic ring xanthorrhizol scaffold formed pi-pi stacking with Trp321. The alkyl side chain also interacted with Tyr247 through pi-alkyl interactions. It has been mentioned that Tyr247, Tyr286 and Trp321 are located near the catalytic cleft of the active site [30].

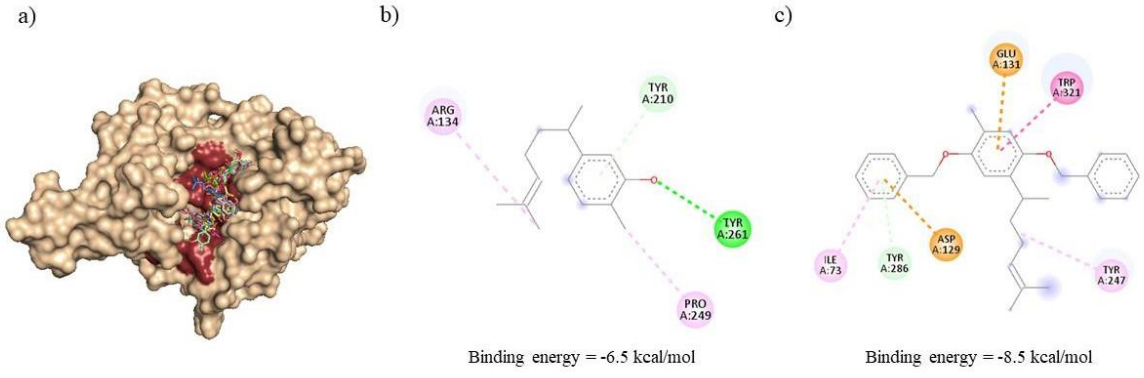

Figure 3. a) The docking poses of all ligands docked against Hyal1. The active site of the Hyal1 enzyme is coloured maroon; 2D representations of amino acid interactions with b) xanthorrhizol, **1**; c) derivative **17**.

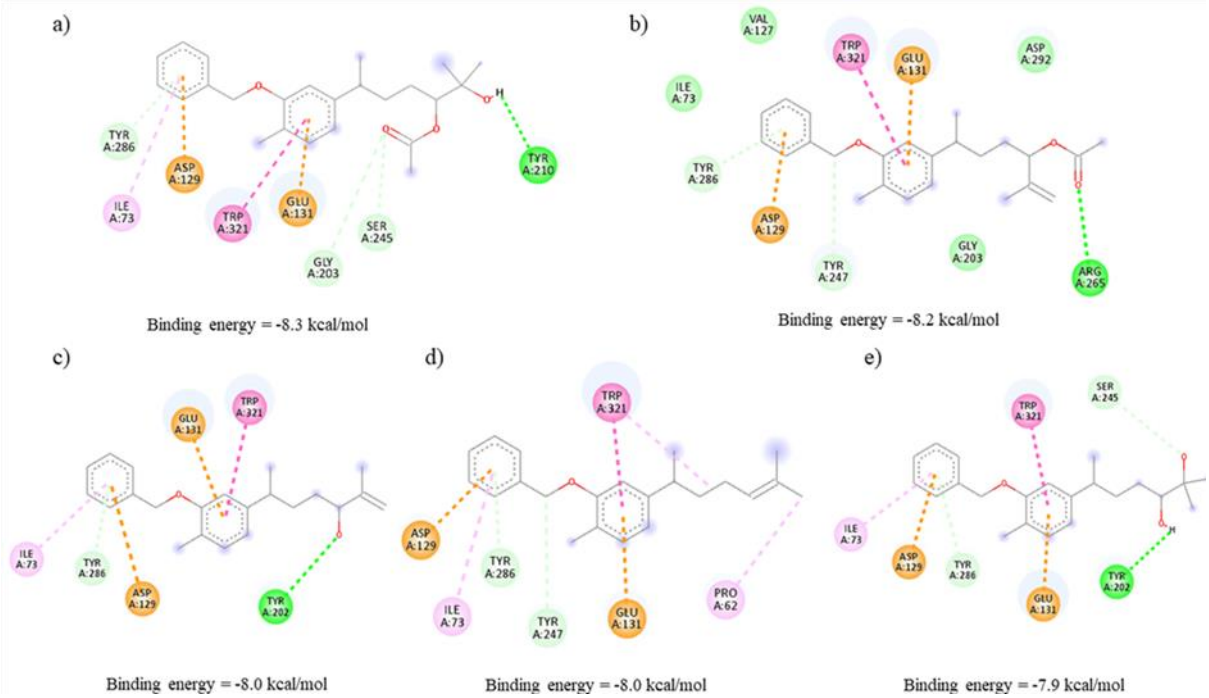

Figure 4. 2D representations of amino acid interactions with a) derivative **24**; b) derivative **25**; c) derivative **11**; d) derivative **15**; and e) derivative **14**.

It is also worth noting that derivatives **24, 25, 11, 15,** and **14** possessed favourable binding energies and interactions despite having only one benzyloxy substituent at R_1 (Figure 4). It can thus be deduced that the presence of the benzyloxy group at R_1 was necessary for Hyal1 inhibitory activity, whereas the benzyloxy group at R_2 had no significant effect on the activity but perhaps provided additional conformational stability to the derivatives.

Substitution of other small functional groups at R_1 such as methoxy (derivatives **10**, **20**, **21**, **22** and **23**), acetate (derivatives **4**, **12** and **13**), and methoxymethyl ether (derivatives **26** and **27**) caused an increase in binding energy, thus reducing the Hyal1 inhibition effect. The presence of small and polar functionalities at R_3 and R_4 positions such as diol (**2** and **3**) or enol (**9**) functionalities gave similar binding energies as xanthorrhizol, implying that these positions had no effect on the Hyal1 enzyme. The negligible influence of the R_3 and R_4 substituents can be further proved by the similar binding energies observed for derivatives **17** and **18**, both with benzyloxy moieties at R_1 and R_2 but differing in their substitutions at R_3 and R_4. Figure 4 provides a summary of the SAR between the xanthorrhizol derivatives and the Hyal1 enzyme.

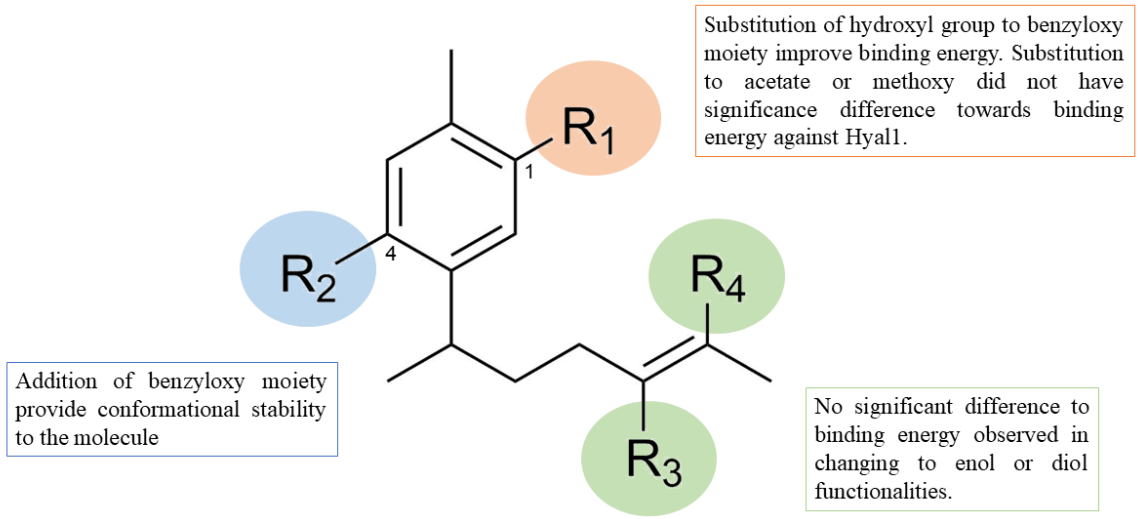

Figure 4. A summary of the SAR between the xanthorrhizol scaffold and Hyal1.

Table 2. Optimum ranges for physicochemical properties as determined by SwissADME.

Descriptors	Range
Lipophilicity (LIPO)	-0.7 ≤ XLOGP3 ≤ +5.0
Molecular weight (SIZE)	150 g/mol ≤ MW ≤ 500 g/mol
Topological polar surface area (POLAR)	20 Å^2 ≤ TPSA ≤ 130 Å^2
Solubility (INSOL)	Log *S* ≥ -6
Carbon bond saturation (INSAT)	Fraction of carbons in the sp^3 hybridization not less than 0.25
Flexibility (FLEX)	0 < Number of rotatable bonds < 9

In silico ADME and Drug-likeness Prediction

SwissADME assessed the compounds' drug-likeness according to the guidelines by Lipinski, Ghose, Veber and Egan [25]. These guidelines shared the same rationale, which was to define the limit for physicochemical parameters by considering six physicochemical descriptors (molecular weight, lipophilicity, solubility, carbon bond saturation, flexibility and topological surface area (TPSA)) [25]. These parameters are important in predicting the ability of xanthorrhizol to be administered and distributed in the human body. The optimum parameter ranges set by SwissADME are shown in Table 2 [25]. Lipophilicity and solubility are important parameters for drug absorption because drug molecules need to pass through both aqueous and hydrophobic environments in the human body [35]. Meanwhile, the presence of rotatable bonds or flexibility in a compound can improve drug permeation as it travels from an aqueous environment to the lipid interior of the plasma membrane. Veber's rule suggests that the number of rotatable bonds should be less than 10 for the drug-likeness criteria [36]. While unsaturation in the compounds helps to improve receptor-ligand complementarity [36], the TPSA value should be less than 120 Å for an orally active drug [37].

Despite having the lowest binding energy, derivative **17** violated the lipophilicity, solubility and TPSA parameters. This may be due to the non-polar functional groups, i.e., two benzyloxy moieties and alkene functionality, which increased its hydrophobicity in comparison with other derivatives. Additionally, the low TPSA value reveals low polarity, leading to poor oral absorption and membrane permeation [38]. The incorporation of polar moieties such as hydroxyl and acetate at R_3 and R_4, as shown by derivatives **14** and **24**, respectively, improved their ADME profiles by increasing the TPSA value. This observation suggests that adding polar functional groups in the xanthorrhizol scaffold is necessary to increase its bioavailability.

Table 3. Molecular weight, sp^3 fraction, number of rotatable bonds, TPSA value, XLOGP and ESOL value of xanthorrhizol and its derivatives.

Derivatives	Molecular weight (150 g/mol ≤ MW ≤ 500 g/mol)	sp^3 fraction (≥0.25)	Number of rotatable bonds (0 < n < 9)	TPSA (20 Å^2 ≤ TPSA ≤ 130 Å^2)	XLOGP (-0.7 ≤ XLOGP3 ≤ +5.0)	ESOL Log S (Log *S* ≥ -6)
1 (Xanthorrhizol)	218.33	0.47	4	20.23	5.46	-4.65
2	252.35	0.6	5	60.69	2.98	-3.2
3	252.35	0.6	5	60.69	2.98	-3.2
4	352.42	0.58	9	93.06	2.41	-3.13
5	268.35	0.6	5	80.92	2.2	-2.79
6	232.32	0.47	4	34.14	4.17	-3.64
7	234.33	0.47	4	40.46	4.67	-4.23
8	448.59	0.38	11	58.92	5.84	-5.98
9	234.33	0.47	5	40.46	4.29	-3.93
10	248.36	0.5	6	29.46	4.18	-3.86

11	324.46	0.36	8	29.46	5.67	-5.27
12	260.37	0.47	6	26.3	5.13	-4.52
13	294.39	0.59	7	66.76	2.66	-3.09
14	342.47	0.45	8	49.69	4.37	-4.54
15	308.46	0.36	7	9.23	6.84	-5.99
16	342.47	0.45	8	49.69	4.37	-4.54
17	414.58	0.31	10	18.46	8.31	-7.42
18	448.59	0.38	11	58.92	5.84	-5.98
19	268.35	0.6	5	80.92	2.2	-2.79
20	232.36	0.5	5	9.23	5.35	-4.58
21	266.38	0.62	6	49.69	2.88	-3.14
22	308.41	0.61	8	55.76	3.45	-3.6
23	290.4	0.5	8	35.53	4.75	-4.32
24	384.51	0.46	10	55.76	4.94	-4.99
25	366.49	0.38	10	35.53	6.25	-5.72
26	296.4	0.65	8	58.92	2.83	-3.14
27	375.3	0.65	8	58.92	3.52	-4.06

*(red = poor, green = good, yellow = intermediate)

Table 4. Predicted Pgp substrate and enzyme inhibition of xanthorrhizol and derivatives **14** and **24**.

Derivatives	Pgp substrate	CYP1A2 inhibitor	CYP2C19 inhibitor	CYP2C9 inhibitor	CYP2D6 inhibitor	CYP3A4 inhibitor
1 (Xanthorrhizol)	No	No	No	Yes	Yes	No
14	Yes	Yes	No	No	Yes	Yes
24	Yes	No	No	No	Yes	Yes

Further analyses of xanthorrhizol and its derivatives (**14**, **24**) were performed to predict their metabolism rate in phase I as a Cytochrome P450 (CYP) enzyme inhibitor and as the Pgp substrate. The Cytochrome P450 (CYP) enzyme superfamily are important for hepatic drug metabolism, while Pgp substrate is a type of drug efflux transporter that functions to limit cellular uptake and increase elimination of drugs into excretion organs [39,40]. As a result, the derivatives were classified as inhibitors for five major CYP isoforms: CYP1A2, CYP2C19, CYP2C9, CYP2D6, and CYP3A4 (Table 4). This indicates xanthorrhizol and its derivatives **14** and **24** were moderately metabolised in the liver as they inhibit only certain CYP isoforms. Furthermore, xanthorrhizol was identified as a non-Pgp substrate while its derivatives **14** and **24** were identified as Pgp substrates. These findings suggest that derivatives **14** and **24** possess good ADME profiles.

CONCLUSION

In conclusion, the SARs of 26 xanthorrhizol derivatives revealed the presence of two benzyloxy moieties at R_1 and R_2 positions, each significantly enhancing the binding activity of the derivative against the Hyal1 enzyme. However, these two hydrophobic moieties also resulted in poor solubility in the human body as shown by the ADME profile of derivative **17**. In contrast, derivatives **14** and **24**, which possessed the most favourable binding energies in the docking studies, conformed with all ADME parameters. This result implies that the presence of polar functional groups in the xanthorrhizol scaffold, especially at the R_3 and R_4 positions, are crucial for good absorption, although the SAR studies indicated they had a minimal effect on binding activity. Nevertheless, this study served as a starting point for the further development and optimization of xanthorrhizol as a scaffold for the Hyal1 enzyme inhibitor. Incorporation of both hydrophobic and polar functional groups containing nitrogen and oxygen atoms in the xanthorrhizol scaffold may improve its binding energy and ADME profile.

ACKNOWLEDGEMENT

The authors gratefully acknowledge financial support from the Fundamental Research Grant Scheme FRGS19-029-0637 (FRGS/1/2018/STG01/UIAM/03/3)

by the Ministry of Higher Education, Malaysia, and the Kulliyyah of Science, International Islamic University Malaysia (IIUM), Kuantan for the research facilities.

REFERENCE

1. Furman, D., Campisi, J., Verdin, E., Carrera-Bastos, P., Targ, S., Franceschi, C., Ferrucci, L., Gilroy, D. W., Fasano, A., Miller, G. W., Miller, A. H., Mantovani, A., Weyand, C. M., Barzilai, N., Goronzy, J. J., Rando, T. A., Effros, R. B., Lucia, A., Kleinstreuer, N. and Slavich, G. M. (2019) Chronic inflammation in the etiology of disease across the life span. *Nature Medicine*, **25(12)**, 1822-1832.

2. Chen, L., Deng, H., Cui, H., Fang, J., Zuo, Z., Deng, J., Li, Y., Wang, X. and Zhao, L. (2018) Inflammatory responses and inflammation-associated diseases in organs. *Oncotarget*, **9(6)**, 7204-7218.

3. Petrey, A. C. and de la Motte, C. A. (2014) Hyaluronan, a crucial regulator of inflammation. *Frontiers in Immunology*, **11(5)**, 1-13.

4. Kaul, A., Short, W. D., Wang, X. and Keswani, S. G. (2021) Hyaluronidases in Human Diseases. *International Journal of Molecular Sciences*, **22(6)**,1-11.

5. Lengers, I., Herrmann, F., le Borgne, M. and Jose, J. (2020) Improved surface display of human Hyal1 and identification of testosterone propionate and chicoric acid as new inhibitors. *Pharmaceuticals*, **13(4)**, 1–18.

6. McQuitty, C. E., Williams, R., Chokshi, S. and Urbani, L. (2020) Immunomodulatory Role of the Extracellular Matrix Within the Liver Disease Microenvironment. *Frontiers in Immunology*, **11**, 574276.

7. Salleh, N. A., Ismail, S. & Ab Halim, M. R. (2016) Effects of *Curcuma xanthorrhiza* Extracts and Their Constituents on Phase II Drug-metabolizing Enzymes Activity. *Pharmacognosy Research*, **8(4)**, 309–315.

8. Yuandani, Jantan, I., Rohani, A. S. and Sumantri, I. B. (2021). Immunomodulatory Effects and Mechanisms of *Curcuma* Species and Their Bioactive Compounds: A Review. *Frontiers in Pharmacology*, **12**, 643119.

9. Jantan, I., Saputri, F. C., Qaisar, M. N. and Buang, F. (2012) Correlation between chemical composition of curcuma domestica and curcuma xanthorrhiza and their antioxidant effect on human low-density lipoprotein oxidation. *Evidence-based Complementary and Alternative Medicine*, **438356**.

10. Rukayadi, Y. and Hwang, J. K. (2006) In vitro activity of xanthorrhizol against Streptococcus mutans biofilms. *Letters in Applied Microbiology*, **42(4)**, 400–404.

11. Rukayadi, Y. and Hwang, J. K. (2013) In vitro activity of xanthorrhizol isolated from the rhizome of Javanese turmeric (Curcuma xanthorrhiza Roxb.) against Candida albicans biofilms. *Phytotherapy Research*, **27(7)**, 1061–1066.

12. Lim, C. S., Jin, D. Q., Mok, H., Oh, S. J., Lee, J. U., Hwang, J. K., Ha, I. and Han, J. S. (2005) Antioxidant and anti-inflammatory activities of xanthorrhizol in hippocampal neurons and primary cultured microglia. *Journal of Neuroscience Research*, **82(6)**, 831–838.

13. Kim, M. B., Kim, C., Song, Y. and Hwang, J. K. (2014) Antihyperglycemic and anti-inflammatory effects of standardized Curcuma xanthorrhiza Roxb. extract and its active compound xanthorrhizol in high-fat diet-induced obese mice. *Evidence-Based Complementary and Alternative Medicine*, **2014**, 205915.

14. Cheah, Y. H., Nordin, F. J., Tee, T. T., Azimahtol, H. L. P., Abdullah, N. R. and Ismail, Z. (2008) Antiproliferative property and apoptotic effect of xanthorrhizol on MDA-MB-231 breast cancer cells. *Anticancer Research*, **28(6A)**, 3677–3689.

15. Lee, S. K., Hong, C. H., Huh, S. K., Kim, S. S., Oh, O. J., Min, H. Y., Park, K. K., Chung, W. Y. and Hwang, J. K. (2002) Suppressive effect of natural sesquiterpenoids on inducible cyclo-oxygenase (COX-2) and nitric oxide synthase (iNOS) activity in mouse macrophage cells. *Journal of Environmental Pathology, Toxicology and Oncology*, **21(2)**, 141–148.

16. Chung, W. Y., Park, J. H., Kim, M. J., Kim, H. O., Hwang, J. K., Lee, S. K. and Park, K. K. (2007) Xanthorrhizol inhibits 12-O-tetradecanoylphorbol-13-acetate-induced acute inflammation and two-stage mouse skin carcinogenesis by blocking the expression of ornithine decarboxylase, cyclooxygenase-2 and inducible nitric oxide synthase through mitogen-activated protein kinases and/or the nuclear factor-kappa B. *Carcinogenesis*, **28(6)**, 1224–1231.

17. Liao, W., Khoo, Y. W., Goh, J. W. K. and Wong, W. -S. F. (2019) Anti-oxidative and anti-inflammatory effects of xanthorrhizol on

aeroallergens-induced biological responses in vitro and ex vivo. *European Respiratory Journal*, **54(63)**, PA4206.

18. Sirat, H. M., Ngai, M. H. and Jauri, M. H. (2007) Chemistry of xanthorrhizol: synthesis of several bisabolane sesquiterpenoids from xanthorrhizol. *Tetrahedron Letters*, **48(3)**, 457–460.

19. Ngai, M. H., and Sirat, H. M. (2004) Synthesis of Bisabolane Sesquiterpenoids from Xanthorrhizol Isolated from C. xanthorrhiza and Their Bioactivities. *Proceeding of the 4th Annual National Science Fellowship Seminar. Vistana Hotel, Penang*, 181–186.

20. Aguilar, M. I., Delgado, G. and Villarreal, M. L. (2001) New bioactive derivatives of xanthorrhizol. *Revista de la Sociedad Química de México*, **45(2)**, 56–59.

21. Rahayu, M. D., Kusumaningrum, S. and Hayun, H. (2020) Synthesis of acetyl and benzoyl esters of xanthorrhizol and its oxidation products and evaluation of their inhibitory activity against nitric oxide production. *International Journal of Applied Pharmaceutics*, 135–138.

22. Hou, T. and Xu, X. (2004) Recent development and application of virtual screening in drug discovery: An overview. *Current Pharmaceutical Design*, **10**, 1011–1033.

23. Ntie-Kang, F. (2013) An in silico evaluation of the ADMET profile of the StreptomeDB database. *Springerplus*, **2(1)**, 1–11.

24. Osakwe, O. (2016) The significance of discovery screening and structure optimization studies. *Social Aspects of Drug Discovery, Development and Commercialization*, 109–128.

25. Daina, A., Michielin, O. and Zoete, V. (2017) SwissADME: a free web tool to evaluate pharmacokinetics, drug-likeness and medicinal chemistry friendliness of small molecules. *Scientific Reports*, **7(1)**, 1–13.

26. Abdullahi, M. and Adeniji, S. E. (2020) In-silico Molecular Docking and ADME/Pharmacokinetic Prediction Studies of Some Novel Carboxamide Derivatives as Anti-tubercular Agents. *Chemistry Africa*, **3(4)**, 989–1000.

27. Cousins, K. R. (2005) ChemDraw Ultra 9.0. CambridgeSoft, 100 CambridgePark Drive, Cambridge, MA 02140. www.cambridgesoft. com.

28. Hanwell, M. D., Curtis, D. E., Lonie, D. C., Vandermeersch, T., Zurek, E. and Hutchison, G. R. (2012) Avogadro: an advanced semantic chemical editor, visualization, and analysis platform. *Journal of Cheminformatics*, **4(1)**, 1–17.

29. Morris, G. M., Huey, R., Lindstrom, W., Sanner, M. F., Belew, R. K., Goodsell, D. S. and Olson, A. J. (2009) AutoDock4 and AutoDockTools4: Automated docking with selective receptor flexibility. *Journal of Computational Chemistry*, **30(16)**, 2785–2791.

30. Chao, K. L., Muthukumar, L. and Herzberg, O. (2007) Structure of human hyaluronidase-1, a hyaluronan hydrolyzing enzyme involved in tumor growth and angiogenesis. *Biochemistry*, **46(23)**, 6911–6920.

31. Trott, O. and Olson, A. J. (2010) AutoDock Vina: improving the speed and accuracy of docking with a new scoring function, efficient optimization, and multithreading. *Journal of Computational Chemistry*, **31(2)**, 455–461.

32. Rahmat, E., Lee, J. and Kang, Y. (2021) Javanese Turmeric (*Curcuma xanthorrhiza* Roxb.): Ethno botany, phytochemistry, biotechnology, and pharmacological activities. *Evidence-Based Complementary and Alternative Medicine: eCAM*, 9960813.

33. Abdullah, N. H., Thomas, N. F., Sivasothy, Y., Lee, V. S., Liew, S. Y., Noorbatcha, I. A. and Awang, K. (2016) Hyaluronidase Inhibitory Activity of Pentacylic Triterpenoids from Prismatomeris tetrandra (Roxb.) K. Schum: Isolation, Synthesis and QSAR Study. *International Journal of Molecular Sciences*, **17(2)**, 1-20.

34. Zhang, L., Bharadwaj, A. G., Casper, A., Barkley, J., Barycki, J. J. and Simpson, M. A. (2009) Hyaluronidase activity of human Hyal1 requires active site acidic and tyrosine residues. *The Journal of Biological Chemistry*, **284(14)**, 9433-9442.

35. Khanna, V. and Ranganathan, S. (2009) Physiochemical property space distribution among human metabolites, drugs and toxins. *BMC Bioinformatics*, **10(15)**, S10.

36. Veber, D. F., Johnson, S. R., Cheng, H. Y., Smith, B. R., Ward, K. W. and Kopple, K. D. (2002) Molecular properties that influence the oral bioavailability of drug candidates. *Journal of Medicinal Chemistry*, **45(12)**, 2615–2623.

37. Kelder, J., Grootenhuis, P. D., Bayada, D. M., Delbressine, L. P. and Ploemen, J. P. (1999) Polar molecular surface as a dominating determinant for oral absorption and brain penetration of drugs. *Pharmaceutical Research*,

16(10), 1514–1519.

38. Rajalakshmi, R., Lalitha, P., Sharma, S. C., Rajiv, A., Chithambharan, A. and Ponnusamy, A. (2021) In Silico studies: Physicochemical properties, drug score, toxicity predictions and molecular docking of organosulphur compounds against Diabetes mellitus. *Journal of Molecular Recognition*, **34(11)**, e2925.

39. McDonnell, A. M. & Dang, C. H. (2013) Basic review of the cytochrome P450 system. *Journal of the Advanced Practitioner in Oncology*, **4(4)**, 263–268.

39. Amin M. L. (2013) P-glycoprotein inhibition for optimal drug delivery. *Drug Target Insights*, **7**, 27–34.